A Hybrid Discontinuous Galerkin-Finite Volume Method for Computational Aeroacoustics

Michael Schlottke-Lakemper, Matthias Meinke and Wolfgang Schröder

Abstract A hybrid method for a fully coupled determination of aerodynamic sound is introduced. From the instantaneous velocity and vorticity, determined by approximate solutions of the Navier-Stokes equations, acoustic source terms are obtained, which are plugged into the acoustic perturbation equations being solved with a high-order discontinuous Galerkin method. The coupling method is discussed in detail and results of validation tests of the aeroacoustics solver are presented.

1 Introduction

Noise reduction is one of the major challenges of today's aircraft development, and together with an increase in fuel efficiency one of the key goals in European aircraft policy. The perceived noise levels of flying aircraft are to be reduced until 2050 by 65 % compared to 2000 [14]. To achieve these goals, efficient, fully parallelized algorithms are needed to predict the far-field noise of jet engines and complete aircraft.

A hybrid large-eddy simulation-computational aeroacoustics method (LES-CAA) for large-scale aeroacoustics simulations exists, [11]. However, this scheme suffers from the limitations of having two separate tools that need to exchange a large data volume via I/O operations. In the new approach, both the LES and CAA solvers are part of the same simulation framework. While the LES solver is based on a finite-volume method for the prediction of the flow field, the CAA approach is based on a high-order discontinuous Galerkin (DG) solver for the acoustic field.

For the coupled LES-CAA solution, first a fully developed flow field has to be obtained by the LES solver. The flow variables are time-averaged to provide mean and perturbed quantities for density, pressure, and velocity. The fluctuating Lamb vector, i.e., the outer product of vorticity and velocity, is then computed at each time

M. Schlottke-Lakemper (✉) · M. Meinke · W. Schröder
Chair of Fluid Dynamics and Institute of Aerodynamics, RWTH Aachen University,
Wüllnerstraße 5a, 52062 Aachen, Germany
e-mail: m.schlottke-lakemper@aia.rwth-aachen.de

step of the LES solver and passed on to the CAA subdomain. The new feature of the hybrid method is that both the LES and CAA solver components are based on a hierarchical Cartesian grid. Both solvers use a joint Cartesian mesh, in which the individual features of the hierarchical grid can be colored to be either pure LES or pure CAA cells or both. A space-filling curve, which operates on the joint mesh, is used to split the domain into subdomains using different weights for the CAA and LES cells. In so doing, subdomains are created for the parallel execution. The coupling between the LES and CAA domains only requires memory transfer operations and no additional communication between subdomains. Thus, the coupling of the two solvers is especially efficient for massively parallel computing systems.

2 Acoustic Perturbation Equations

The acoustic perturbation equations (APE) were introduced in [3] and are used to predict the acoustic field for flow-induced noise. They are derived from the linearized Euler equations (LEE) and modified to retain only acoustic modes without generating vorticity or entropy modes.

Neglecting all viscous, non-linear and entropy-related contributions, the APE-4 system reads [3]

$$\frac{\partial p'}{\partial t} + \bar{c}^2 \nabla \cdot \left(\bar{\rho} u' + \bar{u} \frac{p'}{\bar{c}^2} \right) = 0, \tag{1}$$

$$\frac{\partial u'}{\partial t} + \nabla \left(\bar{u} \cdot u' \right) + \nabla \left(\frac{p'}{\bar{\rho}} \right) = q_m, \tag{2}$$

where the source term q_m is the Lamb vector

$$q_m = -(\omega \times u)'. \tag{3}$$

p is the pressure, u the velocity vector, ω the vorticity vector, ρ the density, and c the speed of sound. The variables of the APE are perturbed quantities denoted by prime $(\cdot)'$ and are defined as $\phi' := \phi - \bar{\phi}$, where the bar $(\bar{\cdot})$ denotes time-averaged quantities.

3 Numerical Methods

3.1 Discontinuous Galerkin Approximation of the APE

A discontinuous Galerkin spectral element method (DGSEM) is used to determine the acoustic field. DG methods were first described in [13] and subsequently applied

to various physical problems. In [12], the DGSEM was proposed and has been used extensively, e.g. in [5, 10].

Since the DGSEM elements correspond to cells in a finite-volume context, the words cell or element can be used interchangeably. In the following sections, an outline of the method is presented. It follows the derivations in [10] but considers the specific characteristics of the used Cartesian grid.

Mapping to reference element A general system of hyperbolic conservation equations in three dimensions reads

$$\frac{\partial \boldsymbol{u}}{\partial t} + \nabla \cdot \boldsymbol{f}(\boldsymbol{u}) = 0, \tag{4}$$

where $\boldsymbol{u} = \boldsymbol{u}(\boldsymbol{x}, t)$ is the vector of conservative variables $\{u_i\}_{i=1}^{n_v}$ and $\boldsymbol{f}$ the flux vector.

For efficiency reasons, the differential equation is mapped to a reference element, which in three dimensions is a cube of size $[-1, 1] \times [-1, 1] \times [-1, 1]$. Introducing the reference coordinate vector $\boldsymbol{\xi} = (\xi, \eta, \zeta)^{\mathsf{T}}$, the final transformed equation reads (c.f. [10])

$$\hat{J} \boldsymbol{u}_t + \nabla_{\boldsymbol{\xi}} \cdot \boldsymbol{f} = 0. \tag{5}$$

$\hat{J}$ is the Jacobian, which in the case of cube-to-cube transformations is just $\frac{h}{2}$, where h is the side length of the cube.

Weak solution The derivation of the DG method starts with the weak form of the equation. Therefore, Eq. 5 is multiplied by a test function $\phi = \phi(\boldsymbol{\xi})$ and integrated over the reference element E,

$$\int_E \left(\hat{J} \boldsymbol{u}_t + \nabla_{\boldsymbol{\xi}} \cdot \boldsymbol{f} \right) \phi \, \mathrm{d}\boldsymbol{\xi} = 0. \tag{6}$$

Using integration by parts on the flux term, we obtain the weak formulation of the differential equation

$$\int_E \hat{J} \boldsymbol{u}_t \phi \, \mathrm{d}\boldsymbol{\xi} + \int_{\partial E} (\boldsymbol{f} \cdot \boldsymbol{n})^* \phi \, \mathrm{d}\boldsymbol{s} - \int_E \boldsymbol{f} \cdot \nabla_{\boldsymbol{\xi}} \phi \, \mathrm{d}\boldsymbol{\xi} = 0, \tag{7}$$

where $\boldsymbol{n}$ is the surface normal vector in the reference system. On the element boundaries ∂E, the value for the normal flux $\boldsymbol{f} \cdot \boldsymbol{n}$ is not unique, since the solutions in the left $\boldsymbol{u}^-$ and right $\boldsymbol{u}^+$ elements are discontinuous, similar to the finite-volume approach. Therefore, a numerical flux $(\boldsymbol{f} \cdot \boldsymbol{n})^* = \boldsymbol{g}(\boldsymbol{u}^+, \boldsymbol{u}^-)$ is chosen that combines values from both sides to a single flux. The local Lax-Friedrichs flux formulations are used. A central scheme with an additional damping factor reads

$$g(u^+, u^-) = \frac{1}{2} \left(f(u^+) + f(u^-) \right) \cdot n + \frac{1}{2} \left(\max_{u \in [u^+, u^-]} |a(u) \cdot n|(u^+ - u^-) \right), \quad (8)$$

where a is the vector of eigenvalues of the flux Jacobian.

Choice of representation The solution u is approximated using a polynomial basis

$$u(\xi, t) \approx \sum_{i,j,k=0}^{N} \bar{u}_{ijk}(t)\psi_{ijk}(\xi), \qquad \psi_{ijk}(\xi) = l_i(\xi)l_j(\eta)l_k(\zeta), \quad (9)$$

where the basis functions ψ_{ijk} are the product of one-dimensional Lagrange polynomials l of degree N in each spatial direction and $\bar{u}_{ijk}(t)$ are the coefficients. The nodal basis is defined on a set of interpolation points $\{\xi\}_{i=0}^{N}$ on the interval $\xi \in [-1, 1]$, which in this work are the Legendre-Gauss nodes (Fig. 1). The fluxes are approximated using the same approach.

Quadrature for surface, volume, and time derivative integrals The three integrals in Eq. 7 are approximated by Gauss quadrature. Generally, Gauss quadrature of an arbitrary function $f(x)$ on the interval $[a, b]$ with $N + 1$ nodes can be written as

$$\int_a^b f(x)\, dx \approx \sum_{i=1}^{N} \omega_i f(x_i), \quad (10)$$

where the weights ω_i and the integration nodes x_i are specific to the chosen quadrature type. These weights are pre-calculated and stored to make the algorithm efficient.

Semi-discrete formulation and time integration With the interpolation points $\{\xi_i\}$ collocated at the Gauss nodes, all sums collapse into single values, yielding the discrete DG operator $\mathcal{L}(u, t) = u_t$ [10]. In the next step, the semi-discrete formulation is integrated in time to obtain the solution at the next time step, for which a low-storage fourth-order Runge-Kutta scheme is used [2].
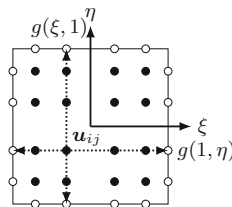

Fig. 1 Legendre-Gauss nodes in a 2D reference element for $N = 3$

3.2 Finite-Volume Method for the Flow Simulation

A second-order in space and time finite-volume method is used to solve the unsteady Navier-Stokes equations for compressible flow. The solver has been extensively validated and used for various flow problems [8, 9]. That is, a more detailed description of the method can be found in the literature.

4 Coupling Strategy

To solve the acoustic perturbation equations, the averaged quantities $\bar{u}$ and $\bar{c}$ and the source term q_m have to be determined first. The flow solution is advanced without coupling until the averaged quantities are statistically converged.

The coupling process can be outlined as follows: (1) advance the LES solution, (2) calculate the source term from instantaneous and averaged quantities, (3) advance the CAA solution. The actual coupling takes place over the source term computed from the LES solution and used in the solver for the APE. This means that there is a one-way coupling from the flow solution to the acoustic field, while the flow solution is not influenced by the acoustic field.

In the following, some details of the coupling method are shown.

4.1 Spatial Coupling

The instantaneous variables of the source term q_m are available after each time step of the flow simulation. They have to be transferred, however, from the flow grid to the acoustics grid. Since both simulations operate on different levels of the same grid, identification of corresponding cells is possible by traversing the octree used for the hierarchical Cartesian mesh. The type of the grid also guarantees that there are no partially overlapping cells, i.e., a smaller cell is always fully contained inside a larger cell. Furthermore, the fact that the DG elements are generally of higher order than the finite-volume cells has to be taken into account. Depending on the resolution of the fluid and acoustics problems, four types of transformations are possible.

One-to-one mapping The simplest case is when one fluid cell corresponds exactly to one acoustics cell (Fig. 2a). In this case, the source term is calculated once in the finite-volume part and the same value is used at all Gauss nodes of the DG element.

One-to-multiple mapping In case there is one fluid cell that is mapped to multiple acoustics cells (Fig. 2b), the procedure is the same as for the 1-to-1 mapping, that is, the source term is calculated once and then used at all Gauss nodes of all elements.
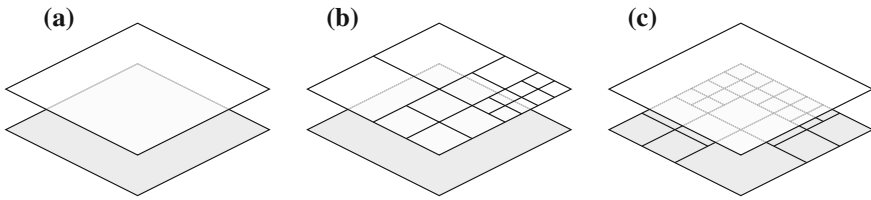
Fig. 2 Possible spatial mappings for coupled simulations. Aeroacoustics cells (*top*) are *white*, fluid cells (*bottom*) are *grey*. **a** One-to-one. **b** One-to-multiple. **c** Multiple-to-one

Multiple-to-one mapping Having multiple finite-volume cells mapped onto one DG element is the most difficult case (Fig. 2c), since the values at the Gauss nodes have to be interpolated from more than one flow cell.

A natural choice would be to interpret the finite-volume cells as equidistant nodes of a polynomial and to obtain the values at the Gauss nodes through projection. This, however, can lead to spurious oscillations if the number of finite-volume cells and thus the polynomial degree is high, especially in regions with large gradients. Other possibilities are weighted least squares methods, nearest neighbor interpolation or inverse distance weighting.

Which approach is the best depends on a number of factors. A practical consideration is the computational cost of the chosen method, e.g., whether the effort scales linearly with the number of degrees of freedom or worse, since the interpolation has to take place at each flow simulation time step. The smoothness of the interpolated function is also important, especially in high-gradient zones. Furthermore, it is desireable to have a conservative interpolation scheme such as proposed in [4], to avoid distorting the source terms.

Unmapped elements If there are regions without either a flow or acoustics grid, no coupling is performed. When only acoustics cells exist, a far-field value for the averaged quantities $\bar{c}$ and $\bar{u}$ has to be specified for the APE, e.g., the freestream values of the flow field. The source term q_m is set to zero with a smooth transition from non-zero to zero values.

4.2 Temporal Coupling

Next, the temporal connection between the flow and acoustics simulations have to be taken into account. Due to the explicit global time stepping, the problem of matching the simulation times has to be solved once for each step.

Equal time step size The simplest approach is when both simulations use the same time step. This can be achieved by determining the next time step in each method and the minimum of both methods is used. In this case, no interpolation of datasets has to be performed.

Different time steps for the fluid and acoustic field Depending on the features of the geometry, the time step for the aeroacoustics simulation may be smaller than for the flow simulation or vice versa, and thus the source terms have to be interpolated between two flow time steps. As for the spatial coupling, there are many different interpolation methods to choose from.

Linear interpolation is the easiest approach, although with often inferior results. In [6], several temporal interpolation methods suitable for hybrid aeroacoustics simulations are compared and evaluated, and least-squares optimized interpolators were found to have the best properties when it comes to broadband error reduction.

4.3 Data Transfer

There are two possibilities of how to transfer data between the flow solution and the acoustics solution: via data files written to disk, i.e., offline coupling, or through in-memory data access, i.e., online coupling.

Offline coupling With offline coupling, the processes of obtaining the flow solution and running the aeroacoustics simulation are completely separated. At first, the flow solution is obtained and the source term q_m is written to a file at certain time intervals. During the acoustics simulation, the source terms are determined from the files by interpolation in time.

Conceptually, this is the simplest approach, since except for the I/O routines nothing has to be changed inside the two simulations. However, the high amount of data that has to be transferred to and from the disk makes this method expensive in terms of computational cost, especially for large-scale simulations on thousands of cores.

Online coupling When online coupling is used, both the flow and the acoustics simulations are fully integrated and run synchroneously at the same time. Typically, the flow solution will be advanced by one time step and the acoustics solution has to be updated until they are both synchronized.

Since no files have to be written to disk, this approach is more efficient than offline coupling. If the acoustics cells are kept on the same computational core as the corresponding flow cells, the acoustics simulation can directly access the relevant information by simple memory transfer operations. This locality of data is achieved by the specific subdomain decomposition, which operates on the joint LES-CAA grid.

On the other hand, the increased memory consumption makes it necessary to use more computational cores. Furthermore, due to the different number of operations for the finite-volume and the DG operator, paired with different numbers of flow cells per acoustics cell, load balancing between the cores becomes mandatory to achieve reasonable parallel efficiency. This is accomplished by assigning appropriate loads to the fluid and acoustics cells.

5   Results

5.1   Hot Coaxial Jet

In Fig. 3, results of an LES of a hot coaxial jet are shown. The solutions were obtained using the finite-volume method described in Sec. 3.2 and are labelled ZFS. The temperature ratio T_p/T_s between the primary (index p) and the secondary (index s) jet is 0.37, while the velocity ratio U_s/U_p is 0.9. The Reynolds number based on the secondary jet conditions is $\mathrm{Re}_s = 400,000$. A 24-million-cell mesh and a maximum resolution of $0.018 h/D$, i.e., cell length per jet diameter, were used. The results for the velocity and turbulence intensity distributions show good agreement with the data from Koh et al. [11].

5.2   Validation of the Aeroacoustics Solver

The results of the aeroacoustics solver show that it is capable of correctly predicting the acoustic field of various validation cases.

Monopole in sheared mean flow Fig. 4 shows the results for wave propagation in a sheared mean flow. An S-shaped velocity profile is prescribed for the mean velocity $\bar{u}$ and an analytical source term generates an acoustic monopole [3]. The DG solution matches the reference solution very well.

Acoustic reflection at solid wall This is the simulation of the reflection of a pressure pulse at a plane wall. The wall boundary conditions are prescribed by setting the mean flow velocity components to zero at wall, $\bar{u} = \bar{v} = 0$, and by enforcing a vanishing perturbed velocity normal to the wall, $n_x u' + n_y v' = 0$. Both the setup and the theoretical values are taken from [7]. The results in Fig. 5 show that the CAA solver is able to correctly predict the propagation of acoustic waves and validate the solid wall boundary conditions.
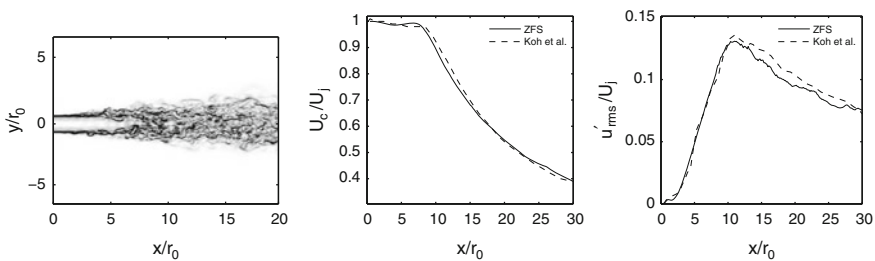

Fig. 3   Hot coaxial jet results for ZFS (—) and Koh et al. [11] (−−) (*left* velocity gradients, *center* centerline velocity, *right* centerline turbulent velocity)
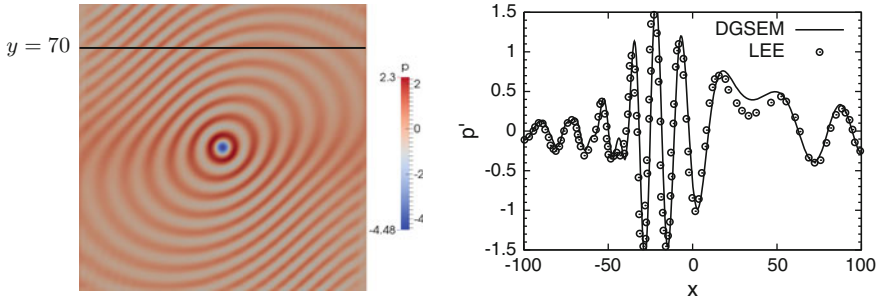
Fig. 4 Monopole in sheared mean flow (*left* perturbed pressure p', *right* comparison of DGSEM with LEE simulation results from [3] for p' at $y = 70$ and $t = 180$)
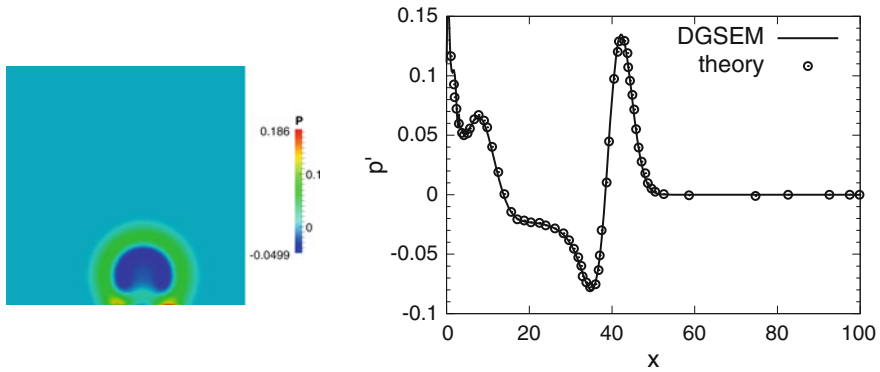

Fig. 5 Reflection of pressure pulse at *solid wall* (*left* perturbed pressure p', *right* comparison of DGSEM with analytical solution from [7] for p' at $x = y$ and $t = 30$)
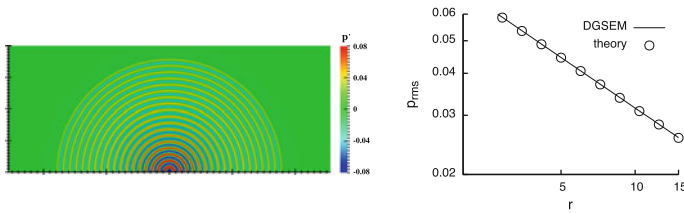

Fig. 6 Monopole in plane wall (*left* perturbed pressure p', *right* rms pressure along y-axis)

Monopole at a solid wall In this case, a plane sound wave is assumed to travel through a small channel and to exit through a small orifice in a plane wall. Due to the small size of the channel, the wave emanating from it is an approximation for a singular monopole at the wall [1]. The reference values in Fig. 6 were obtained

by calculating the theoretical values as the asymptotical far-field solution $p_{\text{RMS}} = A/\sqrt{r}$, where $A = p_{\text{RMS}}\sqrt{r}$ is the amplitude value at $r = 15$. The DGSEM rms pressure distribution perfectly matches the theoretical data.

6 Conclusions

A hybrid approach for large-scale aeroacoustic simulations is described. The flow field is predicted using an LES solver based on the finite-volume method. For the CAA solver, a DG method is used. The coupling of the flow solver and the acoustics solver minimizes the storage requirements and makes the overall LES-CAA approach extremely efficient. Both solvers are validated and the results match the reference data well.

References

1. Bauer, M., Dierke, J., Ewert, R.: Application of a discontinuous Galerkin method to discretize acoustic perturbation equations. AIAA J. **49**(5), 898–908 (2011)
2. Carpenter, M.H., Kennedy, C.: Fourth-order 2N-storage Runge-Kutta schemes. NASA Report TM 109112, NASA Langley Research Center (1994)
3. Ewert, R., Schröder, W.: Acoustic perturbation equations based on flow decomposition via source filtering. J. Comput. Phys. **188**, 365–398 (2003)
4. Farrell, P., Maddison, J.: Conservative interpolation between volume meshes by local Galerkin projection. Comput. Methods Appl. Mech. Eng. **200**(1–4), 89–100 (2011)
5. Flad, D., Frank, H., Beck, A.D., Munz, C.-D.: A discontinuous Galerkin spectral element method for the direct numerical simulation of aeroacoustics. AIAA Paper, pp. 2014–2740 (2014)
6. Geiser, G., Marinc, D., Schröder, W.: Comparison of source reconstruction methods for hybrid aeroacoustic predictions. Int. J. Aeroacoustics **12**(7–8), 639–662 (2014)
7. Hardin, J., Ristorcelli, J.R., Tam, C.K.W. (eds.): ISCASE/LaRC Workshop on Benchmark Problems in Computational Aeroacoustics (CAA), NASA Conference Publication 3000. NASA (1995)
8. Hartmann, D., Meinke, M., Schröder, W.: An adaptive multilevel multigrid formulation for Cartesian hierarchical grid methods. Comput. Fluids **37**, 1103–1125 (2008)
9. Hartmann, D., Meinke, M.: A strictly conservative Cartesian cut-cell method for compressible viscous flows on adaptive grids. Comput. Methods Appl. Mech. Eng. **200**, 1038–1052 (2011)
10. Hindenlang, F., Gassner, G.J., Altmann, C., Beck, A., Staudenmaier, M., Munz, C.-D.: Explicit discontinuous Galerkin methods for unsteady problems. Comput. Fluids **61**, 86–93 (2012)
11. Koh, S., Schröder, W.: Turbulence and heat excited noise sources in single and coaxial jets. J. Sound Vib. **329**, 786–803 (2010)
12. Kopriva, D., Woodruff, S., Hussaini, M.: Discontinuous spectral element approximation of Maxwell's equations. In: Cockburn, B., Kariadakis, G., Shu, C.W. (eds.) Proceedings of the International Symposium on Discontinuous Galerkin Methods. Springer (2000)

13. Reed, W., Hill, T.: Triangular mesh methods for the neutron transport equation. Technical Report LA-UR-73-479, Los Alamos Scientific Laboratory (1973)
14. Directorate-General for Research, Innovation European Union: Flightpath 2050: Europe's Vision for Aviation : Maintaining Global Leadership and Serving Society's Needs. Office for Official Publications of the European Communities (2011)